

## Experimental and Numerical study of the wind flow in a coastal region of the north of Japan

Atsushi YAMAGUCHI<sup>1)</sup>, Takeshi ISHIHARA<sup>1)</sup> and Yozo FUJINO<sup>1)</sup>

1) *Department of Civil Engineering, the University of Tokyo  
7-3-1 Hongo, Bunkyo, Tokyo 113-8656*

### 1 Introduction

For the efficient use of wind energy in Japan, it is very important to predict the wind flow over complex terrains with steep cliffs and slopes. Recently, numerical model is widely used to predict the wind flow over complex terrain. However, numerical simulation includes some uncertainty by numerical method, turbulence model and mesh resolutions. It is necessary to examine how accurate the numerical model can predict the wind flow. To examine the efficiency of the numerical model, it is also important to obtain high-quality experimental data.

Linear model proposed by Jackson and Hunt[1] (JH model) has been widely used for the estimation of wind flow over gentle topography. However, JH model loses its prediction accuracy remarkably when the slope angle is large. Since in the mountain area of Japan the average slope angle is generally large, it is really necessary to develop a non-linear model which can simulate the separation of the flow.

A few study have been done on wind flow with separation over steep terrain by numerical analysis. Coelho and Pereira(1992)[2] and Kobayashi et al.(1994)[3] studied wind flow with separation behind a two-dimensional ridge. Turbulent flows over two ridges or three-dimensional hill were studied by Kim et al.(1997)[4] and Utnes and Eidsvik(1996)[5]. For the wind prediction over real topography, non-linear model was used by Maurizi[6]. Maurizi examined mesh size dependencies on prediction of wind flow by changing mesh size from 200m to 500m, and concluded that prediction error due to mesh size is about 15%. It

is not clear, however, that 200m mesh size is sufficient or not.

In this study, Shakotan Peninsula area, north of Japan, was chosen. The topographic feature of the area is very complex and there are steep cliffs along the north-east coast. We carried out a wind tunnel experiment with 1/2000 scale terrain model to examine the characteristics of wind flow over complex terrain. We also developed CFD based non-linear wind prediction model and compared the prediction results with the wind tunnel experiment. Especially, in this study, we checked how accurately this model can predict the wind and how the mesh size and integral domain size influence the predicted wind flow.



Figure 1: The terrain model used in this study

### 2 Wind tunnel experiment

#### 2.1 Experiment setup

The experiment was carried out in the Wind Engineering Laboratory, the University of Tokyo. Fig.1 shows the terrain model used in this experiment. The scale of the model is 1/2000 and the

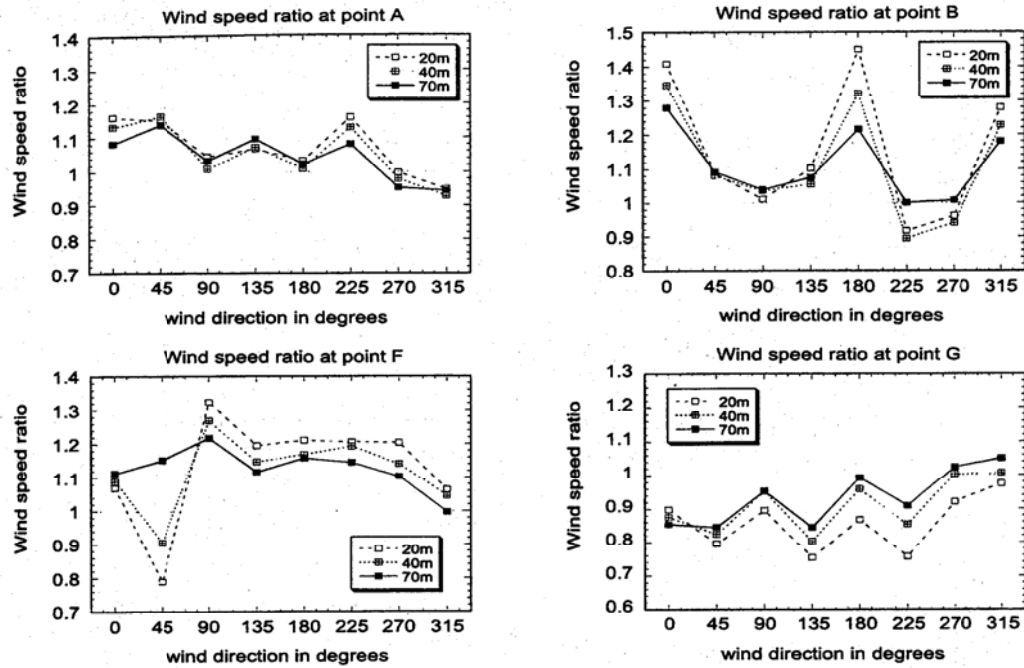


Figure 3: Wind speed ratio at each measurement point



Figure 2: Measurement points

diameter of the model is 4m, which corresponds to 8km in the real scale. The model is installed on a turn table and measurement were performed for the 8 wind directions.

Fig.2 shows the measurement locations. A to G correspond to the wind observation masts described by NEDO[7]. These sites are all located on a plateau except for G, however, the surrounding terrain is different. Around the mast A is relatively flat and less complex. Around the mast B, C and D is a very complex terrain. For the masts E and F, there is a steep cliff with the height of 150m from the sea in northeast side. Mast G is located at a relatively low elevation and surrounded by mountains.

In this experiment, the wind velocity was measured at these seven points at the height of 5mm, 10mm, 20mm, 35mm, 50mm, 75mm, 100mm and 150mm above the ground, which correspond to 10m, 20m, 40m, 70m, 100m, 150m, 200m and

300m in the real scale. Split fiber probe was used to measure longitudinal velocity component. The analogue voltage were low-pass filtered in 500 Hz and digitized in a sampling rate of 1kHz. A sampling time of 20s was used for mean velocities and turbulence statistics.

## 2.2 Experiment result

Fig.3 shows the wind speed ratio at some representative points(point A, B, F and G) at  $z=20\text{m}, 40\text{m}$  and  $70\text{m}$ . The wind speed is defined as  $U/U_0$ , where  $U$  is the mean wind velocity above the terrain and  $U_0$  is the mean wind velocity of the undisturbed flow.

For point A, the wind speed ratio shows relatively small variation with wind direction. This is because surrounding terrain of point A is relatively flat and less complex.

At point B, the surrounding terrain is very complex and the wind speed ratio varies remarkably with the wind direction. The wind speed ratio at  $z=20\text{m}$  reaches almost 1.5 with the southerly wind while it is only around 0.9 with the southwesterly wind. The south side of point B is a valley, which causes the channeling effect and increase in velocity with the southerly wind. When the wind is from southwest, however, the wind direction was forced to change by this valley and as a result, the longitudinal component of the velocity decreases although the magnitude of the velocity increases.

The most striking characteristic of point F is

that the wind speed ratio decreases to 0.8 with the northeasterly wind while it stays around 1.2 with the other wind directions. This is because of the cliff located about 200m away from the point F. The height of the cliff is 150m from the sea. When the wind blows from the northeast, the flow separates at the cliff, which causes low wind speed.

At point G, the wind speed ratio stays lower than 1.0 for almost all the wind directions. This is because point G is at low elevation and surrounded by mountains.

### 3 Numerical Simulation

#### 3.1 Governing equations

Following governing equations were used for the analysis:

$$\frac{\partial \rho u_j}{\partial x_j} = 0, \quad (1)$$

$$\frac{\partial \rho u_j u_i}{\partial x_j} = -\frac{\partial p}{\partial x_i} + \frac{\partial}{\partial x_j} \left( \mu \frac{\partial u_i}{\partial x_j} - \rho \overline{u'_i u'_j} \right), \quad (2)$$

$$\begin{aligned} \frac{\partial \rho u_j k}{\partial x_j} &= \frac{\partial}{\partial x_j} \left[ \left( \mu + \frac{\mu_t}{\sigma_k} \right) \frac{\partial k}{\partial x_j} \right] \\ &\quad - \rho \overline{u'_i u'_j} \frac{\partial u_i}{\partial x_j} - \rho \epsilon, \end{aligned} \quad (3)$$

$$\begin{aligned} \frac{\partial \rho u_j \epsilon}{\partial x_j} &= \frac{\partial}{\partial x_j} \left[ \left( \mu + \frac{\mu_t}{\sigma_\epsilon} \right) \frac{\partial \epsilon}{\partial x_j} \right] \\ &\quad - C_{\epsilon 1} \frac{\epsilon}{k} \rho \overline{u'_i u'_j} \frac{\partial u_i}{\partial x_j} - C_{\epsilon 2} \frac{\rho \epsilon^2}{k}, \end{aligned} \quad (4)$$

where  $u_i$  stands for  $i$  component of the wind velocity,  $p$  for pressure,  $k$  for turbulent kinetic energy,  $\epsilon$  for its dissipation,  $\rho$  for the air density,  $\mu$  for the laminar viscosity coefficient and  $\mu_t$  for the turbulent viscosity coefficient. To approximate the Reynolds stress, standard  $k$ - $\epsilon$  model was used.

#### 3.2 Numerical scheme

To suit the computation of complex flow, the arbitrary non-orthogonal collocated grid system is used. The governing equations are rewritten in the curvilinear coordinate system and are solved using a common discrete method[8]. In this study, finite volume method and the SIMPLE algorithm are adopted. The QUICK scheme is employed for the convection terms in the Navier-Stokes equations, the first order upwind difference for the convection terms in the equations of  $k$  and  $\epsilon$ , and the second-order central difference for the other terms. The Rhie and Chow's PWIM (pressure weighted interpolation method) is used to avoid pressure-velocity decoupling.

### 3.3 Numerical result

To examine how the numerical results depend on the integral domain, two and three dimensional calculations were carried out. Fig.4 shows the domain for the three dimensional calculation. The dashed line in the figure shows the cross section with which two dimensional calculation was carried out.

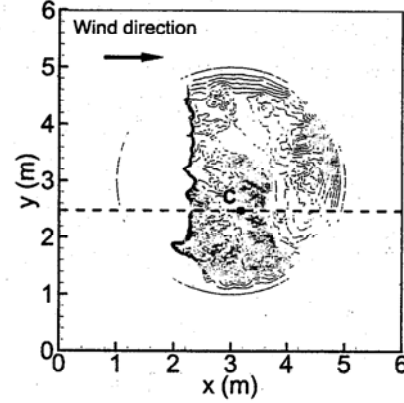


Figure 4: integral domain

Fig.5 shows the vertical profile of the calculated mean wind velocity  $U$  at point C. The two dimensional calculation overestimates the wind velocity while the three dimensional calculation shows good agreement with the experiment results. This is because of the existence of the wind which flows around the terrain model, although the hill height is much smaller than the model width. All the following calculation is three dimensional.

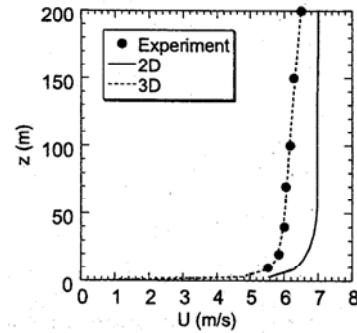


Figure 5:  $U$  profile at pt.C, NE wind

To examine adequate size of mesh to predict wind flow, three different grids were used. The mesh interval of each grid is 100m, 50m and 25m.

Fig.6 shows the mean velocity vectors of flow field in each case. It is clear that 100m grid cannot simulate the flow separation behind the cliff. This is because the steep cliff itself cannot be described by 100m grid. The results with the other two grids

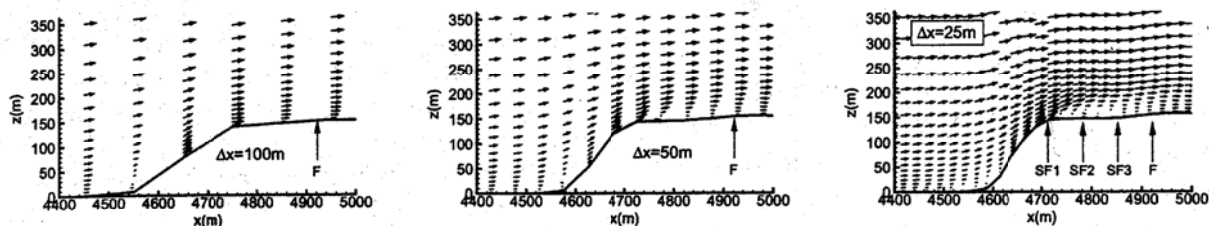


Figure 6: Calculated flow with different mesh

show the flow separation clearly.

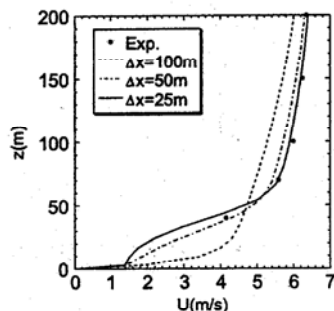


Figure 7:  $U$  profile at pt.F, NE wind

Fig.7 shows vertical profile of  $u$  component of velocity at point F. The wind speed profile from the simulation with 100m mesh is considerably different from other profiles because the flow separation cannot be reproduced by 100m mesh at the cliff. Both 25m and 50m mesh results can predict the flow separation and the 25m mesh result shows slightly better agreement with the experiment.

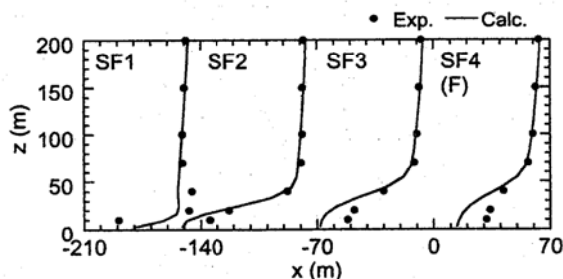


Figure 8:  $U$  profile around pt.F, NE wind

Fig.8 shows the mean wind speed profile for the northeasterly wind around point F. The points SF1 to SF3 is located on the upstream of point F and their positions are shown in Fig.6. This non-linear model can predict the wind speed decrease due to the flow separation but shows slower recovery of the wind speed behind the separation area.

Fig.9 shows the comparison of the measured and predicted mean wind speed at all the measurement point for the northeast wind at  $z=40m$

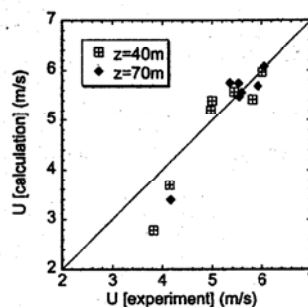


Figure 9: Comparison of measured and predicted wind speed

and 70m. The measured and predicted wind speed show good agreement generally. However, at point G, the predicted wind speed shows lower value than measured wind speed.

#### 4 Conclusion

Wind speed characteristics on a complex terrain was investigated by wind tunnel experiment. Wind speed decrease by a flow separation at the cliff and increase by three dimensionality of the terrain was made clear. The wind field over the complex terrain was also investigated by non-linear model. Numerical results give a fairly good agreement with the wind tunnel experiment. For the typical terrain in Japan, at least 50m mesh is necessary to simulate the flow separation at the cliff.

#### References

- [1] P. S. Jackson and J. C. R. Hunt, Quart. J. R. Met. Soc., Vol. 101, 1975.
- [2] P. J. Coelho and J. C. F. Pereira, Int. J. Num. Methods Fluids, Vol. 14, 1992.
- [3] Kobayashi, M. H. Pereira, J. C. F. and Siqueira, M. B. B., J. Wind Eng. and Ind. Aero., Vol. 53, 1994.
- [4] H. J. Kim, C. M. Lee, H. C. Lim, and N. H. Kyong, J. Wind Eng. and Ind. Aero., Vol. 66, 1997.
- [5] Utnes, T. and Eidsvik, K. J., Boundary-Layer Meteorol. Vol. 79, 1996.
- [6] A. Maurizi, J. M. L. M. Palma and F. A. Castro, J. Wind Eng. and Ind. Aero., Vol. 74-76, 1998.
- [7] NEDO "Evaluation of the wind resource prediction models", 1998 (in Japanese)
- [8] Ishihara, T. and Hibi, K., J. Wind Eng., No. 83, 2000 (in Japanese)

key words: wind energy, complex terrain, CFD, non-linear model